Non-invasive long-term and real-time analysis of endocrine cells on micro-electrode arrays

Matthieu Raoux, Yannick Bornat, Adam Quotb, Bogdan Catargi, Sylvie Renaud, Jochen Lang

Non-invasive long-term and real-time analysis of endocrine cells on micro-electrode arrays

Matthieu Raoux[1,2], Yannick Bornat[3], Adam Quotb[3], Bogdan Catargi[1,4], Sylvie Renaud[3], Jochen Lang[1,2]

[1] Univ. Bordeaux, CBMN, UMR 5248, F-33600 Pessac, France

[2] CNRS, CBMN, UMR 5248, F-33600 Pessac, France

[3] Univ. Bordeaux, IMS, UMR 5218, F-33400 Talence, France

[4] Centre Hospitalier Universitaire de Bordeaux, Service d'endocrinologie.

Non-technical Summary

Pancreatic islet cells are required for glucose homeostasis and their dysfunction leads to diabetes mellitus. The electrical activity of these cells is regulated by nutrients as well as hormones and this provides the first integrative read-out reflecting their function. Non-invasive recording of their electrical activity and its analysis in real time would provide the possibility of long-term and repetitive investigations or testing of multiple drugs. Combining electrophysiology and microelectronics, we now demonstrate such an approach with multiple (up to 60) electrodes and including on-line signal analysis on the two major cell types present in islets, α- and β-cells. This method should be applicable to other endocrine cells and may serve in the long-run as the basis for a novel biosensor.

Word count of the summary: 120

ABSTRACT

Non-invasive high-throughput and long-term monitoring of endocrine cells is important for drug research, phenotyping, tissue engineering and pre-transplantation quality control. Here we report a novel approach to obtain simultaneous long-term electrical recordings of different islet cell types using multi-electrode arrays. We implemented wavelet transforms to resolve the low signal/noise ratio inherent to these measurements and extracted on-line a signature specific of cell activity. The architecture employed allows multiplexing a large number of electrodes for high-throughput screening. This method should be of considerable advantage in endocrine research and may be extended to other excitable cells previously not accessible to the technique.

Abbreviations: ASIC, Application-specific integrated circuit; FPGA, field-programmable gate array; SWT, stationary wavelet transform; MEA, multi-electrode array.

Running Title: Long-term and real-time analysis of endocrine cells

INTRODUCTION

Glucose homeostasis requires insulin secretion from β-cells clustered in a micro-organ, the pancreatic islets. They are regulated by nutrients and further tuned by hormones to reflect the physiological needs of the organism (Henquin, 2000). Ensuing membrane depolarization and action potentials provide the first integrative read-out reflecting the state of these cells (Hiriart & Aguilar-Bryan, 2008). Derangements in glucose homeostasis are a hallmark of diabetes mellitus, a currently incurable and costly disease that is characterized by dysfunction of islets. On-line large-scale monitoring of islets would be of considerable advantage to assess function prior to transplantation, to screen compounds, to phenotype transgenic mice or to follow differentiation of stem-cells. Most approaches beyond hormone secretion are invasive, requiring probe loading thus precluding long-term or repetitive measurements. Genetically encoded sensors allow long-term recordings (Palmer *et al.*, 2011) but major problems persist such as probe bleaching, expansive computing time and difficulties in pattern recognition (Schroeder, 2011). They may also be biased by a fixed genetic background and size of recorders or light sources restrict miniaturization. In contrast, monitoring electrical activity provides information without prior specific manipulation and is suited for real-time analysis and miniaturization in the case of implantation. Extracellular recordings preserve the cell's plasma membrane, a prerequisite for signals driven by metabolism and long-term observations. Their major disadvantage resides in their very low signal-to-noise ratio especially in endocrine cells and in the generation of huge amounts of data during prolonged recordings. To resolve these two problems, we developed a new screening device and novel real-time signal processing by integrated circuits based on submicron technologies.

METHODS

Preparation of islets and cell culture. Experiments were performed on mouse islet cells or clonal β-cells cultured for 2-7 days on MEAs (MEA100/10-Ti-gr, Multichannel Systems, Reuttlingen, Germany) coated with Matrigel (BD Biosciences, San Diego, USA) or on poly-D-lysine/laminin-coated glass coverslips. Mice were sacrificed by stunning and cervical dislocation and islets were obtained as described and approved by the ethics committee (Roger *et al.*, 2011). Cells from 80-100 or 20-40 islets were seeded and cultured at 11 mmol/l glucose. Clonal β-cells INS-1E cells were generously provided by P. Maechler and C. B. Wollheim (Université de Genève, Switzerland) and cultured as published (Roger *et al.*, 2011).

Electrophysiology. Whole-cell perforated patch-clamp recordings in current-clamp configuration were performed at 33°C using an EPC-9 amplifier (HEKA, Lambrecht, Germany). Data were acquired and analysed with Patchmaster (v2.35, HEKA) and IGOR Pro (v6.04, Wavemetrics, Lake Oswego, OR). Patch pipettes pulled from borosilicate glass capillaries had tip resistances of 2–4 MΩ when filled with the internal solution containing (in mM): K_2SO_4 76, NaCl 10, KCl 10, MgCl 2.1, and HEPES 5 (pH 7.35 with KOH). The external solution was (in mM): NaCl 135, KCl 4.8, $MgCl_2$ 1.2, $CaCl_2$ 2.5, HEPES 10, and glucose as indicated (pH 7.4 adjusted with NaOH). Zero-current potential was adjusted in the bath and electrical contact with the cell interior established by addition of amphotericin B (0.24 mg/ml) to the internal solution. Extracellular recordings with MEAs were performed at 37°C with the same external solution as above. For experiments with primary cells, this solution was gassed with O_2/CO_2 (94%/6%) before pH adjustment and enriched with 0.1% (m/v) of bovine serum albumin. A MEA1060-Inv-BC-Standard amplifier was used for these recordings and simultaneous analogue data were acquired at 10 kHz per electrode with MC_Rack™ software (Multichannel Systems, Reuttlingen, Germany).

Spike detection using hardware: Detection was implemented on a configurable digital integrated circuit (FPGA) in 90 nm technology from Xilinx™ (Spartan 3E XC3S500E; San Jose, CA, USA), using the VHDL hardware description language and the Xilinx *ISE* design tool for synthesis. Spikes are detected by comparison with a threshold set as a multiple of the standard deviation σ of the recorded signal after its processing by a stationary wavelet transform. Due to limited occurrence and small amplitudes of spikes, we approximate the probability of the signal to exceed σ to 0.159, which is the equivalent probability for a Gaussian white noise having a mean of zero. That actual probability is obtained by averaging (using a low-pass filter) the duty cycle of a comparator output and the following inputs: 1) the recorded signal without its DC component ($d^1[n]$ after SWT, see figure 3.b); 2) the actual σ value. σ is servoed to 0.159 using a feedback loop. A low-pass filter and an amplifier respectively smooth and multiply σ by a factor K. The threshold $K \times \sigma$ is applied to the i^{th} decomposition level by the SWT of the input signal. The detection output is an asynchronous binary signal (high-level for $d^1[n] > \sigma$ low-level for $d^1[n] < \sigma$). Experimental results in figure 3 were obtained with K=4 and i =6.

Spike detection using software. The threshold module of the MC_Rack™ software was used for off-line spike detection (in Fig. 1 and Fig. 3c). Data were digitally filtered between 10 and 1000 Hz except for the condition named “software” in Fig. 3c (7-3000 Hz). For each channel

the threshold was set to six times the standard deviation of the average noise amplitude in the absence of spikes. The dead time, which represents the absolute refractory period, was set to 40 ms.

Statistics. Results are presented as mean ±S.E.M. Paired Student's *t* tests were used or ANOVA with Bonferroni's as post hoc test for comparisons between 2 groups or more. **p*<0.05; ***p*<0.01, ****p*<0.001.

RESULTS

Figure 1*A* gives the general outline of our approach. Clonal β-cells or primary islet cells are cultured on micro-electrode arrays (MEA) that contain multiple plates to record electrical signals. Electrical signals were conditioned, recognized and first sampled off-line. We subsequently developed Application Specific Integrated Circuits (ASICs) on FPGAs and implemented stationary wavelets for real-time on-line treatment. Electrical activity of islet cells is generally recorded using sharp electrodes or patch clamp which do, however, not permit long-term recordings. Moreover, patch clamp requires a specific and time-consuming configuration, the perforated patch, to prevent dilution of metabolic signals into the micropipette. This complex patch configuration records well the glucose-induced increase in membrane potential and subsequent firing of action potentials (Fig. 1*B*). Non-invasive recordings using extracellular electrodes present a major advantage in terms of success rate and long-term monitoring. In contrast to neurons or cardiomyocytes, action potentials in β-cells do generally not extend beyond 0 mV and these cells will thus exhibit only minute field potentials. Despite this challenge, we were able to capture glucose-induced generation of field potentials by extracellular recordings on MEA electrodes (Fig. 1*B*). Spike frequencies measured with MEAs were in the same order as those in patch-clamp (1.96±0.39 and 2.00±0.53 Hz, respectively, n=3-9). As pancreatic islet cells have never been recorded previously on MEAs we first evaluated relevant biological parameters before implementing novel signal detection functions. Glucose effects on spike frequencies in INS1-E clonal β-cells were dose-dependent for concentrations mimicking hyperglycaemia (> 5.5 mM) as well as hypoglycaemia (< 5.5 mM) (Fig. 1*C*). The set-up also captured the effects of hormones that physiologically regulate islets: firing rates of clonal β cells in the presence of elevated glucose were increased by the intestinal hormone GLP-1 (Fig. 1*D*). Moreover, spike frequencies increased reversibly and repetitively in response to increased glucose concentrations (Fig. 1*E*) without deterioration of the recordings as occurs during patch-clamp. Long-term monitoring

of cells was feasible as documented here for the effect of prolonged exposure to elevated glucose concentrations on clonal β-cells termed glucotoxicity (Roger *et al.*, 2011) (Fig. 1*F*). Most importantly, the device allowed for the first time simultaneous electrophysiological recordings of different islet cell types on the same biological sample as shown here for α- and β-cells (Fig. 1*G*) which were differentiated by the effect of adrenalin (Dean and Matthews, 1970; De Marinis et al., 2010). We further validated the suitability of the device for drug screening using compounds targeting islet cell ion channels (Braun *et al.*, 2008) (Fig. 1*H*). As expected, electrical signals from mouse β cells were inhibited by the L-type Ca^{2+}-channel blocker nifedipine and increased by the K^{+}-channel blockers iberiotoxin, tetraethyl ammonium, and stromatoxine-1. The N-type Ca^{2+}-channel blocker ω-conotoxin GVIA had no detectable effects (not shown). Tetrodotoxin-sensitive Na^{+}-channels were involved in glucose-induced action potentials in mouse β-cells as previously published for human cells (Braun *et al.*, 2008). Previous experiences in mouse β-cells using patch-clamp revealed the presence of these channels but it was concluded that they do not contribute to glucose-induced action potentials (Plant, 1988). For real-time on-line analysis, electrode analogue voltage signals have to be conditioned, digitized, and finally processed for spike detection by integrated electronics in real-time that is less than 5 μs delay. To this end we designed ASICs which ensure ultra-high speed spike detection coping with real-time constraints and variations of signal baseline as well as signal amplitude. We also established novel signal detection functions to minimize computational delays and large data storage. This ensures real-time online analysis when multiplexing the detecting devices and miniaturization for in-vivo use. The inhomogeneity and the non-stationary character of discrete biological time series imply several fundamental steps: centring, denoising, smoothing to single out signal trends and subsequent focusing on impulse characteristics. Consequently we first developed on-line computing of adaptive thresholds depending on signal standard deviation. Second, as wavelet transforms provide compression and time–frequency localization for feature extraction (Phillies, 1996), they are particularly well suited for detection of signals with low signal/noise ratio as encountered here. We optimized stationary wavelet transforms, which supply excellent time-frequency filters in accordance with the characteristics of action potentials (Fig. 2). Haar and beta mother wavelets provided the highest detection rate. The Haar wavelet was used in the study as it represents the simplest relevant wavelet and thus requires less computing time. Moreover, using ASICs, stationary wavelet transforms for up to 70 recorded signals can still be time-multiplexed on a single computational channel thus facilitating real-time processing in screening (Fig. S1).

The procedure and its experimental validation are illustrated by testing on very noisy recordings (Fig. 3). Each recorded signal is digitized and processed by a stationary wavelet transform SWT (Kyung Hwan & Sung June, 2003) (Fig. 3*A*). The first decomposition level of the signal ($d^1(n)$) is used to compute on-line an adaptive threshold and applied for spike detection of the absolute value of $d^6(n)$, the 6th decomposition level of $x[n]$. We implemented an algorithm that adaptively sets a detection threshold to capture action potentials and to reject occasional background peaks. Due to the low frequency and duration of spikes, the standard deviation σ (equal to its root mean square) of the signal approximates the standard deviation of Gaussian white noise having a mean of zero. By definition the probability P for such a signal to be larger than σ is *0.159*. We implemented a digital ASIC on FPGA (Fig. 3*B*) that computes: i) the stationary wavelet transform; ii) σ using a servo loop referenced to probability P=0.159; iii) a dynamic spike detection function whose threshold is the multiple of σ by a factor M. As in white Gaussian noise 95% of samples locate between 0 and 3σ, setting M to 3 ensured correct spike detection. The values of P and M can be modified depending on estimated signal distribution and signal-to-noise ratio. Our newly designed on-line circuit performed similar or better than the off-line software (the latter setting the optimum attainable) in differential spike recognition between basal and elevated glucose concentrations (Fig. 3*C*). Moreover, our circuit provides the major advantages of real-time processing and of significantly less silicon area for its hardware integration thus minimizing fabrication costs and power consumption.

DISCUSSION

The novel technology developed here records the regulation of a micro-organ implicated in diabetes. Using CMOS compatible electrode arrays, we have designed a low power/low cost integrated system able to quantify and decode the detected parameters on-line. Its low heat generation and power dissipation, important to preserve biological samples, compares favourably with imaging techniques (Schroeder, 2011). Multiplexing and long-term recordings, up to at least several days, generates huge amounts of information. Their efficient on-line handling is guaranteed by the specific properties of the integrated circuit in terms of signal identification and computed final data out-put at a defined significance level. Although similar devices have been presented previously (Imfeld *et al.*, 2009; Jones *et al.*, 2011), they only worked off-line and on considerably larger signals such as those recorded here. During the submission of our manuscript a similar electrophysiological approach was reported by

Pfeiffer et al. recording the effect of glucose on islets positioned on one microelectrode of a multi-array and using fraction of plateau phase of the sustained bursting phase as signal read-out (Pfeiffer et al., 2011). This read-out and overall approach does not allow real-time analysis and may become even more computing-time intensive if not only one electrode of the array is used or long-term recordings are performed.

Our approach presented here may be extended to other excitable cells previously not accessible to the technique. In the long term this may allow its use as an embedded system and serve as bio-microelectronic hybrid sensor of the metabolic status in small animals (Raoux et al., 2011).

ACKNOWLEDGMENTS

This work was supported by a grant from the Région Aquitaine (within the program "Delivrer" to BC, SR and JL), from the ANR (HY-Biopacs, to JL and SR), the CNRS (program Longévité to JL and SR) and funding from the University of Bordeaux 1 (JL, SR and AQ). M.R. was supported by a personal grant from the French Diabetes Society (SFD). We gratefully acknowledge J. Gaitan and C. Blatche for perfect technical assistance.

AUTHOR CONTRIBUTIONS

J.L. and S.R. initiated the project as principal investigators, obtained funding, designed experiments and wrote the manuscript. B.C. participated in fund raising and provided critical input to potential clinical applications. M.R., Y.B. and A.Q. conceived experiments, designed and performed experiments, analysed data and wrote the manuscript.

REFERENCES

Braun M, Ramracheya R, Bengtsson M, Zhang Q, Karanauskaite J, Partridge C, Johnson PR & Rorsman P. (2008). Voltage-gated ion channels in human pancreatic beta-cells: electrophysiological characterization and role in insulin secretion. *Diabetes* **57,** 1618-1628.

Dean PM & Matthews EK. (1970). Electrical activity in pancreatic islet cells: effect of ions. *J Physiol* **210:** 265-275

De Marinis YZ, Salehi A, Ward CE, Zhang Q, Abdulkader F, Bengtsson M, Braha O, Braun M, Ramracheya R, Amisten S, Habib AM, Moritoh Y, Zhang E, Reimann F, Rosengren AH, Shibasaki T, Gribble F, Renström E, Seino S, Eliasson L & Rorsman P. (2010). GLP-1 inhibits and adrenaline stimulates glucagon release by differential modulation of N- and L-type Ca^{2+} channel-dependent exocytosis. *Cell Metabolism* **11**: 543-553

Henquin JC. (2000). Triggering and amplifying pathways of regulation of insulin secretion by glucose. *Diabetes* **49,** 1751-1760.

Hiriart M & Aguilar-Bryan L. (2008). Channel regulation of glucose sensing in the pancreatic beta-cell. *Am J Physiol Endocrinol Metab* **295,** E1298-1306.

Imfeld K, Maccione A, Gandolfo M, Martinoia S, Farine PA, Koudelka-Hep M & Berdondini L. (2009). Real-time signal processing for high-density microelectrode array systems. *Int J Adapt Con Sign Proc* 23. 983-998.

Jones IL, Livi P, Lewandowska MK, Fiscella M, Roscic B & Hierlemann A. (2011). The potential of microelectrode arrays and microelectronics for biomedical research and diagnostics. *Anal Bioanal Chem* **399,** 2313-2329.

Kyung Hwan K & Sung June K. (2003). A wavelet-based method for action potential detection from extracellular neural signal recording with low signal-to-noise ratio. *IEEE Transactions on Biomedical Engineering* **50,** 999-1011.

Palmer AE, Qin Y, Park JG & McCombs JE. (2011). Design and application of genetically encoded biosensors. *Trends Biotechnol* **29,** 144-152.

Pfeiffer T, Kraushaar U, Dufer M, Schonecker S, Haspel D, Gunther E, Drews G, Krippeit-Drews P. (2011). Rapid functional evaluation of beta-cells by extracellular

recording of membrane potential oscillations with microelectrode arrays. *Pflugers Arch* **462:** 835-840

Phillies GDJ. (1996). Wavelets: A New Alternative to Fourier Transforms. *Comput Physics* **10,** 247-252

Plant TD. (1988) Na^+ currents in cultured mouse pancreatic B-cells. *Pflugers Arch* **411:** 429-435

Raoux M, Bontorin G, Bornat Y, Lang J, Renaud S. (2011). Bioelectronic sensing of insulin demand. In *Biohybrid Systems - Nerves, Interfaces and Machines*, Jung R (ed). Wiley-VCH, Weinheim, FRG.

Roger B, Papin J, Vacher P, Raoux M, Mulot A, Dubois M, Kerr-Conte J, Voy BH, Pattou F, Charpentier G, Jonas JC, Moustaid-Moussa N & Lang J. (2011). Adenylyl cyclase 8 is central to glucagon-like peptide 1 signalling and effects of chronically elevated glucose in rat and human pancreatic beta cells. *Diabetologia* **54,** 390-402.

Schroeder T. (2011). Long-term single-cell imaging of mammalian stem cells. *Nat Meth* **8,** S30-S35.

FIGURE LEGENDS

Figure 1: Bio-electronic acquisition system and characterization of electrical activities of clonal β-cells and mouse islet cells

A, Architecture: 2-days old culture of mouse islet cells on an electrode array; microelectrodes at the centre of the ring are connected to output contact pads at the device periphery. Spike detection is processed using either off-line detection a standard software tool or on-line detection an application specific integrated circuits (ASIC) in commercial Complementary Metal Oxide-Semiconductor (CMOS) technology. *B*, Upper panel: Representative intracellular perforated patch-clamp recording (current clamp) of a primary β-cell. In response to an increase of glucose concentrations from 3 to 15 mM (G15, horizontal bar), the cell depolarized and subsequently generated sequences of spikes of ~50 mV in amplitude. Lower panel: Representative extracellular recording of glucose-evoked electrical activity generated by primary β-cells cultured on one of the 60 MEA electrodes. *C*, Glucose concentration-dependent firing rate of clonal β-cells. The concentration of glucose was increased every 10 min to mimic hyperglycaemia (> 5.5 mM) and subsequently decreased to mimic

hypoglycaemia (<5.5 mM). Normalized mean frequencies (n=4-12) were determined over 5 min. *D*, Firing rates of clonal β-cells in the presence of 5.5 mM glucose, 15 mM glucose and 15 mM glucose with 10 nM GLP-1 (G15+GLP-1). Mean frequencies (n=18) were determined during the early phase (1 min) of the response. *E*, Clonal β-cells reproducibly changed their firing rates over 110 min under repetitive changes in the external glucose concentrations from 5.5 to 15 mM. Upper panel: representative recording of 5.5 mM or 15 mM glucose (5.5, 15) applied alternatively during 10 minutes; lower panel: mean spike frequencies (n=22) were determined over the last 5 min for each condition before each change in the glucose concentration. *F*, Chronically elevated glucose reduces the electrical activity of clonal β-cells. Cells were cultured in the presence of 11 mM glucose for 3 days and firing rates determined in the presence of 3 and 15 mM glucose. Subsequently the same cells were further cultured for 3 days at 11 mM (G11, left panel) or 20 mM (G20, right panel) glucose at the end of which firing rates for G3 and G15 were again recorded (normalized mean frequencies, n=27-111). *G*, Simultaneous recordings of mouse primary α-cells (n=18) and β-cells (n=36) identified on the same MEAs (glucose 5 or 15 mM; A, 5 μM adrenaline). *H*, Effects of ion channel modulating drugs on glucose-induced (G15) electrical activities of primary mouse islet cells: glucose 5 or 15 mM (5, 15), nifedipine (N, 25 μM, n=18), iberiotoxin (I, 100 nM, n=12), tetraethyl ammonium chloride (TEA, 20 mM, n=12), stromatoxin-1 (STX, 100 nM, n=12), tetrodotoxin (TTX, 500 nM, n=3). Horizontal and vertical scales in panel *E* and *G and H* represent 3 min and 30 μV, respectively.

Figure 2: Mothers wavelets and their performance in correct detection of spikes recorded on microelectrode arrays from β-cells

A, Names and shapes of 5 mother wavelets tested in our circuit (db4, Daubechies 4; ior1.3: biorthogonal 1.3; sym2: Symlet 2; beta: a mother wavelet we created to detect spikes from clonal β-cells; haar: Haar or Daubechies D2 wavelet). *B,* Comparison of detection of clonal β-cell activity with different mother wavelets (n=50, original recording time = 1.8s). Haar and beta mother wavelets provided the highest detection rate. The Haar wavelet was used in the study as it represents the simplest possible wavelet and thus requires less computing time.

Figure 3: On-line adaptive spike detection of β-cell activity recorded by MEAs

A, Noise filtering and signal compression by Stationary Wavelet Transforms (SWT) that process signals from β-cell activity recorded as shown in Fig. 1. 6-level SWT detection on the right panel shows the timing of the spikes as detected by the comparator (block C1, panel *B*). *n* is the filters level, *G* a high-pass filter, *H* a low-pass filter; *x(n)* the digitized input signal; $d^i(n)$ the signal output at the i^{th} decomposition level. The 6^{th} level decomposition output $d^6(n)$ is the reference signal for spike detection using the adaptive threshold circuit in *B*. *B*, adaptive threshold circuit for spike detection (left panel) after noise filtering as described in *A* and final read-out (right panel) of the trace presented in *A*. The entire detection circuit was implemented into an ASIC, a digital configurable integrated circuit (FPGA). The signal recorded on an electrode is digitized into *x(n)* using a 12-bits analogue-to-digital converter (not shown). SWT is implemented as in *A*. The absolute value of $d^6(n)$, the 6^{th} decomposition level of *x(n)*, is compared to a dynamically computed threshold *T* using the comparator block *B*. $d^6(n)$ is high-pass filtered by *G* and has a null mean value. If we servo, using a feedback loop, the duty cycle of the signal (obtained using a low-pass filter *F1*) to *0.159* after comparison with σ (comparator *C1*), V_σ is set to the RMS level of the input waveform. *G1* gain in the feedback loop is used for normalization. σ is smoothed by the *F2* filter and amplified by *G2*, thus setting the detection threshold *T* to (σ x *G2*). *C*, spike detection statistics demonstrate that circuit performances are equivalent or better than the software results. Clonal β-cells were recorded on the MEA set-up and signals were processed using either 1) the MC_Rack software (*software*), 2) the same software after digital filtering (*software after filtering*) or 3) the integrated detection circuit as described in *B* (*wavelet circuit*). 1) and 2) were realized off-line whereas detection using the circuit in 3) was realized on-line and in real time. Experiments using low and high glucose concentrations were analysed (3 mM, G3, N=37; 15mM, G15; N=18). Left panel: mean spike frequencies determined at G3 and G15

with the 3 methods. Right panel: performances of each method in terms of percentages of correct/false detections comparing G3, G15 and pooled data (G3 and G15, termed Global). Validation of each spike was finally controlled visually. **, $p<0.01$, ***, $p<0.001$ as compared to the condition "*software"*.

FIGURE 1

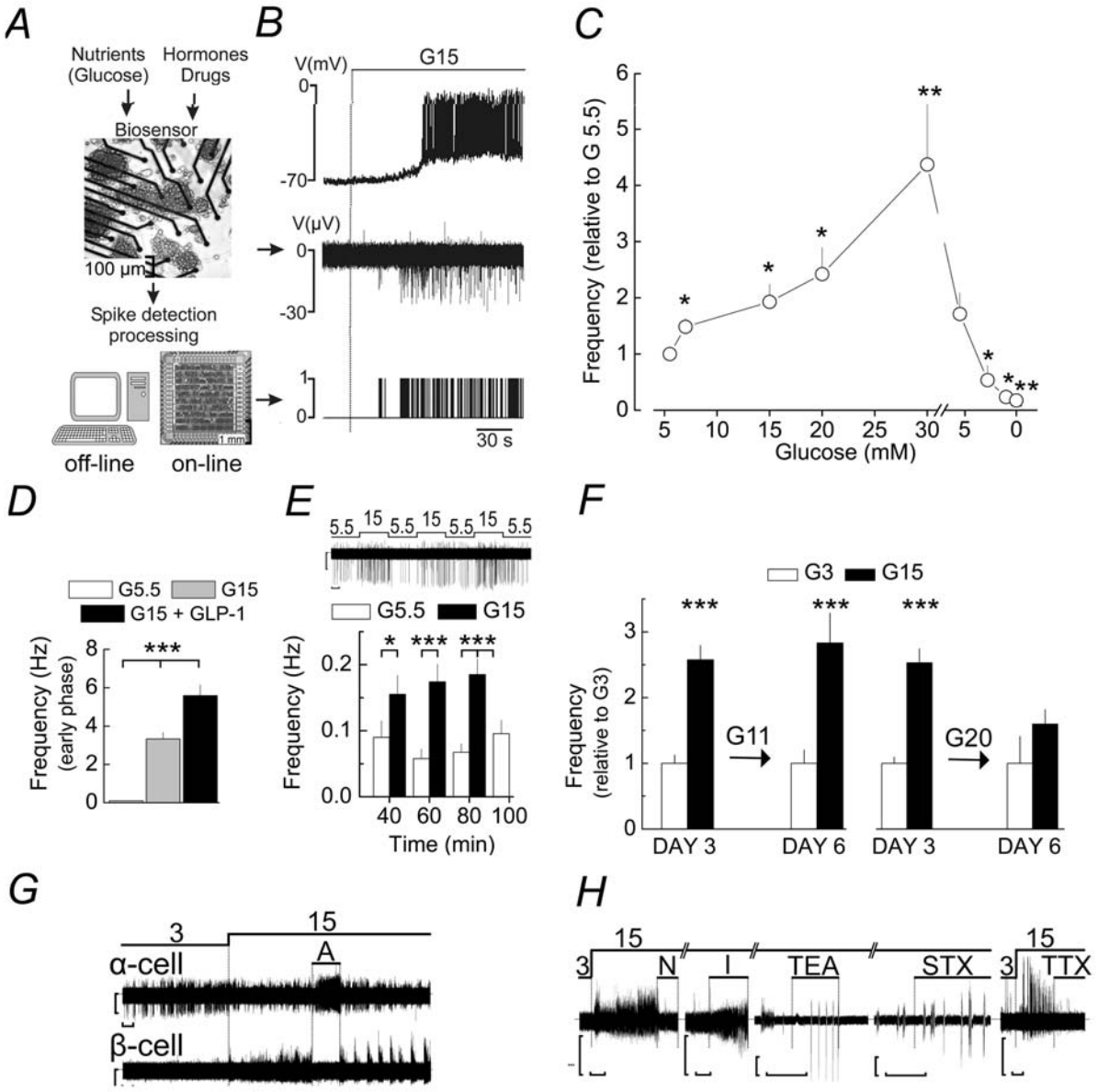
A
Nutrients (Glucose)
Hormones Drugs
Biosensor
100 µm
Spike detection processing
1 mm
off-line
on-line
B
V(mV)
G15
0
-70
V(µV)
0
-30
1
0
30 s
C
Frequency (relative to G 5.5)
Glucose (mM)
5 10 15 20 25 30 5 0
D
G5.5
G15
G15 + GLP-1
Frequency (Hz) (early phase)
***
E
5.5 15 5.5 15 5.5 15 5.5
G5.5
G15
Frequency (Hz)
* *** ***
Time (min)
40 60 80 100
F
G3
G15
Frequency (relative to G3)
***
G11
G20
DAY 3
DAY 6
G
3
15
α-cell
A
β-cell
H
15
3
N
I
TEA
STX
TTX

FIGURE 2

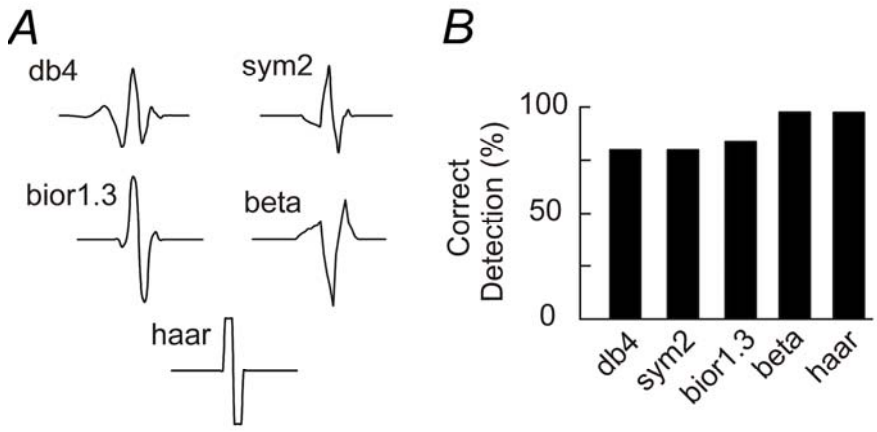

FIGURE 3

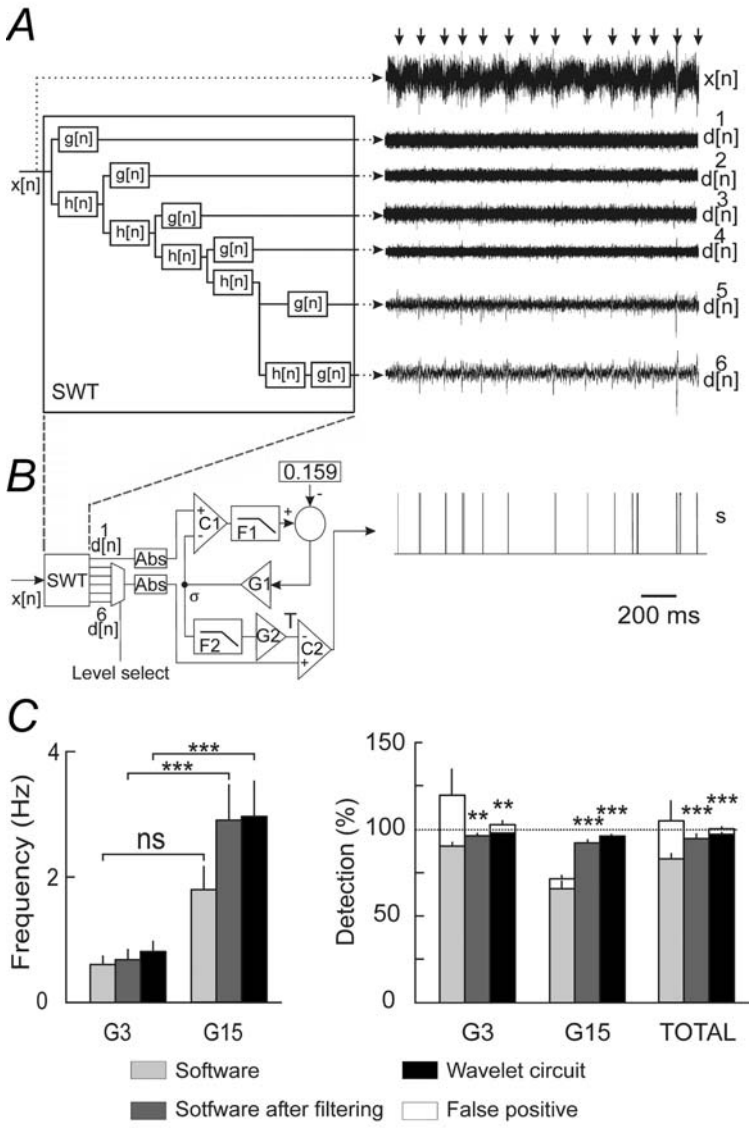

SUPPLEMENTAL FIGURE

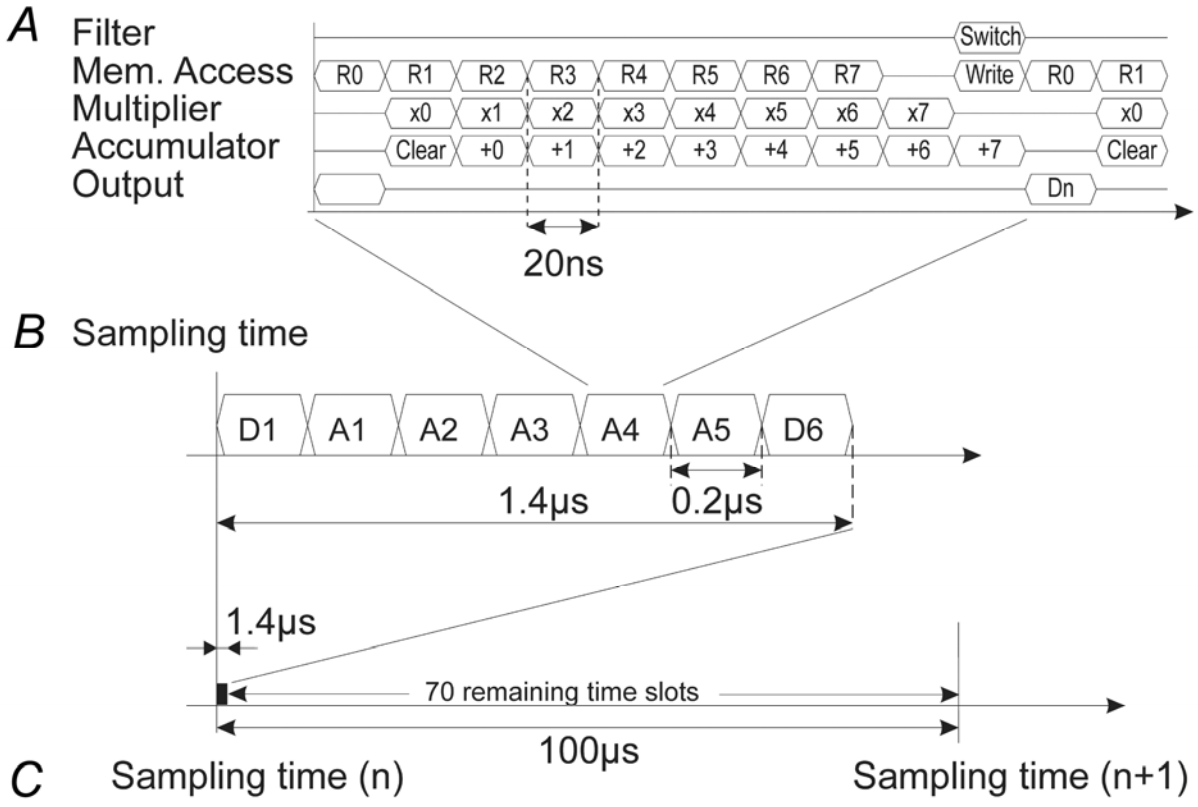

Figure S1: Stationary Wavelet Transform (SWT) computation timing

A, Operation sequence for one level of decomposition in SWT: 10 clock cycles (20 ns each) are necessary to calculate the output *Dn.* Four functional units are involved into the computation: multiplexing filter, static memory (SRAM), multiplier and accumulator.

B, The 6th level of decomposition of SWT is available after a series of 6 cycles as in *A*, i.e. 1.4µs. *C,* All experiments were conducted with a 10 kHz sampling frequency on the recorded biological signal. SWT computation on 1 sample is 1.4 µs, meaning that up to 70 equivalent computations can be conducted using the same functional circuit during the 100 µs period between 2 samples. This demonstrates that SWT for 70 recorded signals can be time-multiplexed on a single computational channel, still ensuring real-time processing.